JMEPEG (2008) 17:96–100
DOI: 10.1007/s11665-007-9111-6

©ASM International
1059-9495/$19.00

Electrochemical Corrosion Study of Tin-based Solders in Potassium Formate Brines for Heat Transfer Applications

Mingzhang Wang and Satish C. Mohapatra

(Submitted May 2, 2006; in revised form February 12, 2007)

Electrochemical corrosion tests were performed on various tin-based solder alloys in stirred potassium formate solutions, pH = 8 and 10.5, with or without additives of corrosion inhibitor, between 20 °C and 75 °C. Open circuit and corrosion potentials and corrosion rates were measured, and galvanic corrosion of the tin-silver solder/copper couples was evaluated. The effects of pH and inhibitor on corrosion of tin-based solder alloys were also assessed.

Keywords electrochemical corrosion, heat transfer fluids, lead-free solders, potassium formate

1. Introduction

Solder is one of the important materials used in heat transfer (heating and cooling) systems. There are mainly two categories of solders, i.e., lead-based and lead-free solders. The latter has become increasingly important for industrial applications, since an international effort has been made to develop and characterize lead-free solders for replacing traditional Pb-Sn solders as a consequence of governmental regulations and marketing pressure concerning health and environmental hazards of lead (Ref 1-2). Currently available lead-free solders are mostly high-tin alloys, including Sn-Ag, Sn-Cu, Sn-Sb, Sn-Zn, Sn-Ag-Cu, and Sn-Ag-Cu-Sb. Microstructure, metallurgical, mechanical and physical properties of lead-free solders have been studied by various groups (Ref 3-7). There are also some investigations on corrosion and electrochemical behavior of lead-free solders in water (Ref 8), salt solutions (Ref 9-11), and acids (Ref 12).

Solder joints in heat transfer systems can be susceptible to corrosion due to direct contact with heat transfer fluids. Failure may occur as leaking through corroded solder joints. The mechanisms can be general corrosion, localized corrosion (e.g., pitting, crevice), and/or galvanic corrosion of dissimilar metals (e.g., solder and substrate). Improper soldering (e.g., flux remains and gaps between soldered parts) can also affect the corrosion process. Thus, understanding of corrosion of solder in heat transfer fluids is needed for the design and materials selection of heat transfer systems. Among heat transfer fluids, potassium formate brines are nontoxic and nonflammable, and have high thermal conductivity, high specific heat capacity and low freezing point, which makes them suitable for many low temperature cooling and heating applications.

In this study, electrochemical corrosion behavior of four tin-based solder alloys, SnAg4, SnAg5.5, SnSb5, and SnCu5Ag2Sb2 were tested in heat transfer fluids based on potassium formate solutions, at different pH, temperature and corrosion inhibition (inhibited vs. uninhibited). The SnAg4 solder was studied in more detail. Galvanic corrosion of the SnAg4 solder and copper couples was evaluated.

2. Experimental Procedure

The tin-based solder alloys used in this study were SnAg4, SnAg5.5, SnSb5, and SnCu5Ag2Sb2. The specimens were cut and straightened from commercially available wire (about 3.2 mm in diameter) spools made by different manufacturers. The area to be tested was about 4 cm^2. The area not to be tested was isolated using Teflon tube and 3M epoxy adhesive DP-460 (off-white, cured at room temperature).

The copper ($Cu > 99.99\%$, machined rod) specimens used for galvanic corrosion tests were about 12.7 mm in length and 9.5 mm in diameter with a threaded hole in the center of one end for electrode connection (which is a standard design of test coupons according to ASTM G5), made by Metal Samples Company (Munford, AL).

Table 1 listed the alloy composition, density, valence, and equivalent weight (EW) used in the tests. Note that the alloy composition and density were obtained from the manufacturers' MSDS sheets and websites. For elements with multiple valences, the valence mostly occurred was chosen to calculate the equivalent weight.

The specimens were polished with SiC (600 and 1200 grit) papers and cleaned with Kimwipes in tap water, rinsed with ultra pure water (17.6 MΩ-cm) and alcohol, and then dried and measured before testing. The tested specimens may be repolished to use again, if there was no pitting in previous test or the pits can be easily removed by repolishing.

The solutions used for testing were made of 49% potassium formate and deionized water with pH adjusted by formic acid and/or potassium hydroxide, which were (i) solution #1 with additives of corrosion inhibitor, Dynalene® HCA+HCB, and pH = 10.5, (ii) solution #2 without additives of corrosion inhibitor and pH = 10.5, and (iii) solution #3 with the same

Mingzhang Wang, and **Satish C. Mohapatra,** Dynalene, Inc, 5250 West Coplay Road, Whitehall, PA 18052. Contact e-mail: mingw@dynalene.com.

additives of corrosion inhibitor and pH = 8, respectively (see Table 2).

Tafel scans were performed in the solutions (without deaeration or aeration) at different temperatures (20-75 °C) in a water bath with a magnetic stirring rate of 400 RPM. A SCE reference electrode (without salt bridge) and a high-purity graphite rod counter electrode were used in several tests in the beginning of the study. Then a saturated Ag/AgCl reference electrode (with a salt bridge) and a platinum wire counter electrode were used for most of the tests lately. The change was made to avoid possible contamination of the reference electrode and the electrolyte, and did not have any notable effects in the test results. The potentiodynamic scan rate was 0.4 mV/s (for most of the tests) and 1 mV/s (in a few tests for comparison). A Gamry (Warminster, PA) PCI4 system available with a corrosion cell kit and DC105 software was used to control the tests, record the data, and measure the open-circuit potential (E_{oc}), corrosion potential (E_{corr}), corrosion current density (i_{corr}), and corrosion rate (CR). The test procedure was basically complied with ASTM G5 (except that the electrodes, the electrolytes, and the testing conditions were as specified above), and the calculation of corrosion rate was in accordance with ASTM G102.

Galvanic corrosion tests of SnAg4 solder and copper couples were performed using the same system in ZRA (zero resistance ammeter) mode, and galvanic current and potential were recorded.

3. Test Results and Discussion

Electrochemical corrosion test results of various solder specimens in the solution #1 at 25 and 50 °C and in the solutions #2 and #3 at 25 °C were listed in Table 2. The potentials in Table 2 have been converted and referred to NHE by subtracting the potential difference between the reference electrode and the standard hydrogen electrode, without considering potential shift (if any) due to the temperature dependence and thermal liquid junction (Ref 13) of the reference electrode. The open-circuit potentials of all the specimens (including copper) were plotted in Fig. 1a, and the corrosion potentials of SnAg4 and copper specimens and their galvanic potentials were shown in Fig. 1b. The general corrosion rates obtained from Tafel scans were shown in Fig. 2a, and the galvanic corrosion test results were presented in Fig. 2b. Some of the potentiodynamic scan curves were shown in Fig. 3. For the two potentiodynamic scan rates (0.4 and 1 mV/s) used, there was no obvious effect in corrosion potentials and corrosion rates, but the lower scan rate did give a clearer display of passivation behavior.

3.1 Open-Circuit Potential and Corrosion Potential

The open-circuit potentials (E_{oc}) of all solder specimens were lower than those of copper (Fig. 1a). This means that the solder specimens would be anodic when galvanically coupled to copper, and galvanic corrosion would occur (see section 2.4). The E_{oc} of solders slightly decreased with the increase in temperature. Yet the temperature dependence of E_{oc} of copper was very small. The difference of E_{oc} between solder and copper thus increased with temperature.

The corrosion potentials (E_{corr}) measured from Tafel scans were generally lower than corresponding E_{oc} (Fig. 2b). The shift between E_{corr} and E_{oc} could be related to the change in surface conditions of specimens during the potentiodynamic scanning. For example, an inhibition film formed on the surface could be changed with increasing potential from cathodic to

Table 1 Alloy composition, density, valence, and equivalent weight of solder and copper specimens

Alloy Composition	Density, g/cm^3	Valence	Equivalent Weight
SnAg4	7.36	Sn (4+), Ag (1+)	30.56
SnAg5.5	7.39	Sn (4+), Ag (1+)	30.91
SnSb5	7.24	Sn (4+), Sb (5+)	30.84
SnCu5Ag2Sb2	7.10	Sn (4+), Cu (2+), Ag (1+), Sb (5+)	30.08
Cu	8.96	Cu (2+)	31.77

Table 2 Electrochemical corrosion test data (average) of solders at 25 °C and 50 °C

Solutions (#)			SnAg4		SnAg5.5		SnSb5		SnCu5Ag2Sb2	
pH	Inhibitor	Alloy Results	25 °C	50 °C	25 °C	50 °C	25 °C	50 °C	25 °C	50 °C
10.5	Yes (#1)	E_{oc}, V vs. V_{NHE}	−0.32	−0.42	−0.41	−0.47	−0.40	−0.48	−0.40	−0.48
		E_{corr}, V vs. V_{NHE}	−0.42	−0.59	−0.56	−0.49	−0.55	−0.63	−0.53	−0.62
		i_{corr}, μA/cm^2	0.26	0.80	0.09	3.01	0.07	3.89	0.08	4.39
		CR, μm/year	3.47	10.81	1.27	41.27	0.96	54.23	1.16	60.94
10.5	No (#2)	E_{oc}, V vs. V_{NHE}	−0.50	···	−0.49	···	−0.41	···	−0.45	···
		E_{corr}, V vs. V_{NHE}	−0.60	···	−0.59	···	−0.48	···	−0.54	···
		i_{corr}, μA/cm^2	1.31	···	0.62	···	0.32	···	0.26	···
		CR, μm/year	17.85	···	8.46	···	4.44	···	3.65	···
8	Yes (#3)	E_{oc}, V vs. V_{NHE}	−0.43	···	−0.40	···	−0.37	···	−0.35	···
		E_{corr}, V vs. V_{NHE}	−0.57	···	−0.55	···	−0.47	···	−0.42	···
		i_{corr}, μA/cm^2	16.27		11.55	···	0.17	···	0.16	···
		CR, μm/year	221.43	···	158.29	···	2.34	···	2.28	···

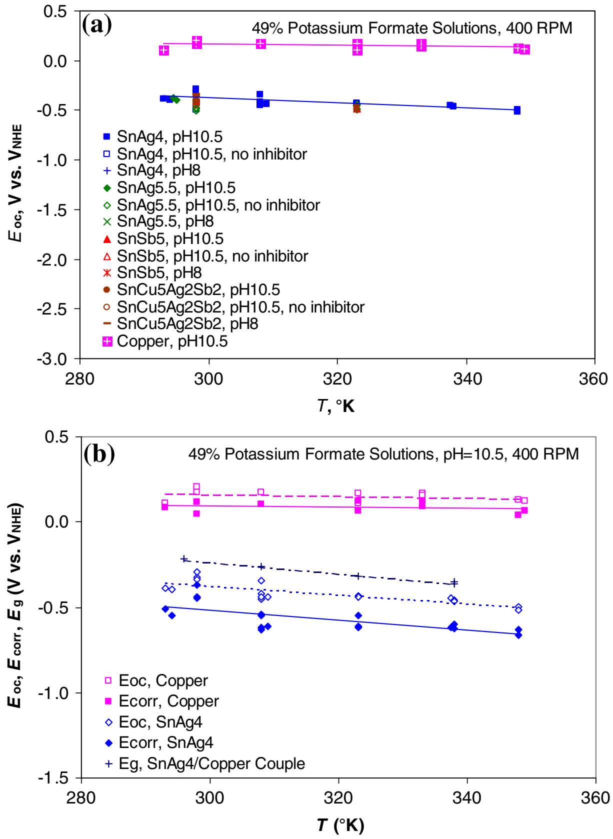

Fig. 1 (a) Open-circuit potentials (E_{oc}) of solders and copper; (b) Open-circuit potential (E_{oc}), corrosion potential (E_{corr}) and galvanic potential (E_g) of SnAg4 and copper. The solutions were inhibited (except specified) and stirred (400 RPM)

anodic. The shift down of E_{corr} of SnAg4 was greater than that of copper. The temperature dependence of E_{corr} was similar to that of E_{oc} of each material.

Among the four tin-based solder alloys, the difference in the open-circuit potentials or corrosion potentials in each solution was small.

3.2 General Corrosion Rate and Effects of pH and Inhibitor

For the solution of pH = 10.5 with inhibitor (solution #1), the corrosion rates of all the tin-based solders fell in the same range of values (Table 2, Fig. 2), and can be rated as Outstanding (<25 μm/year) at 25 °C and Excellent (25-100 μm/year) at 50 °C according to Table 1.3 of (Ref 14). However, from the test results of SnAg4 (see line in Fig. 2), the rating of corrosion rates could be reduced to Good (100-500 μm/year) or Fair (500-1000 μm/year) at 65 and 75 °C. SnAg4 had a lowest corrosion rate at 50 °C in comparison to other solder alloys.

For the solution of pH=10.5 without inhibitor (solution #2), the corrosion rates of all the solders at 25 °C can be still rated as Outstanding, but they were 3-7 times higher than those in the solution #1 and expected to be even higher at higher temperature.

For the solution of pH=8 with inhibitor (solution #3), the corrosion rates at 25 °C can be rated as Outstanding for tin-antimony and tin-copper-silver-antimony solders, but only Good for both tin-silver solders.

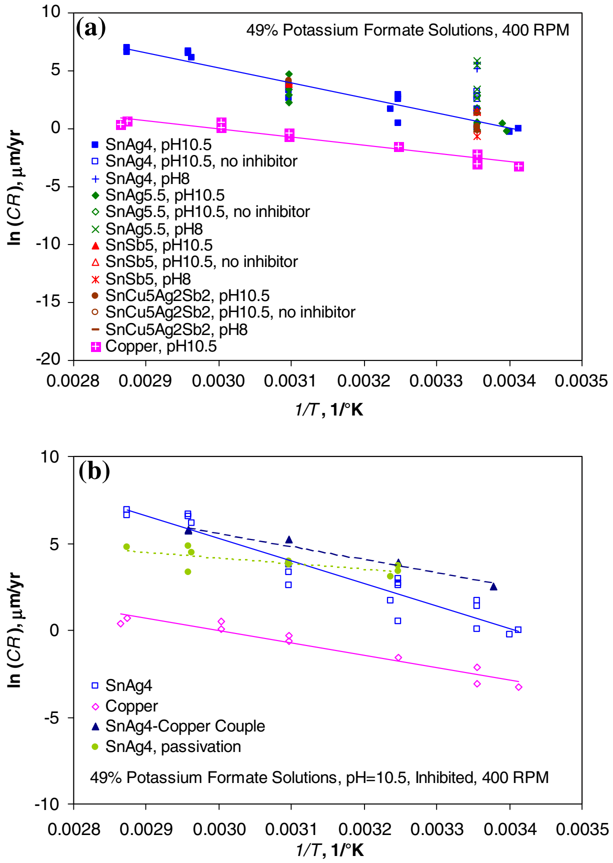

Fig. 2 (a) General corrosion rates of solders and copper in different solutions; (b) General corrosion rates and galvanic corrosion rates of SnAg4 and copper, and corrosion rates calculated from passivation current of SnAg4, in solution #1

Thus, it is clear that for tin-based solder alloys the solution of pH ~ 10.5 worked much better than that of pH = 8. The lower pH value was very harmful to tin-silver solders, as compared to those with antimony and/or copper in replace of silver.

The addition of inhibitor was effective to improve corrosion performance of the solution (corrosion rates of solders in solution #1 vs. those in #2). However, as temperature went up, the corrosion rates of solders increased rapidly (Table 2, Fig. 2). Investigation of various inhibitors may be needed when temperature is up to 65 °C or above.

3.3 Temperature Dependence of General Corrosion Rate

As seen in Fig. 2, the temperature dependence of corrosion rate (CR) of both the solder (SnAg4) and copper can be roughly described by the following Arrhenius type equations respectively, since the corrosion rate was calculated from corrosion current density which was an indication of corrosion reaction rate (Ref 14):

$$(\mathrm{CR})_{\mathrm{solder}} = 7.62 \times 10^{18} \cdot \exp\left[-\frac{1.06 \times 10^5}{RT}\right] (\mu\mathrm{m/year}), \qquad \text{(Eq 1)}$$

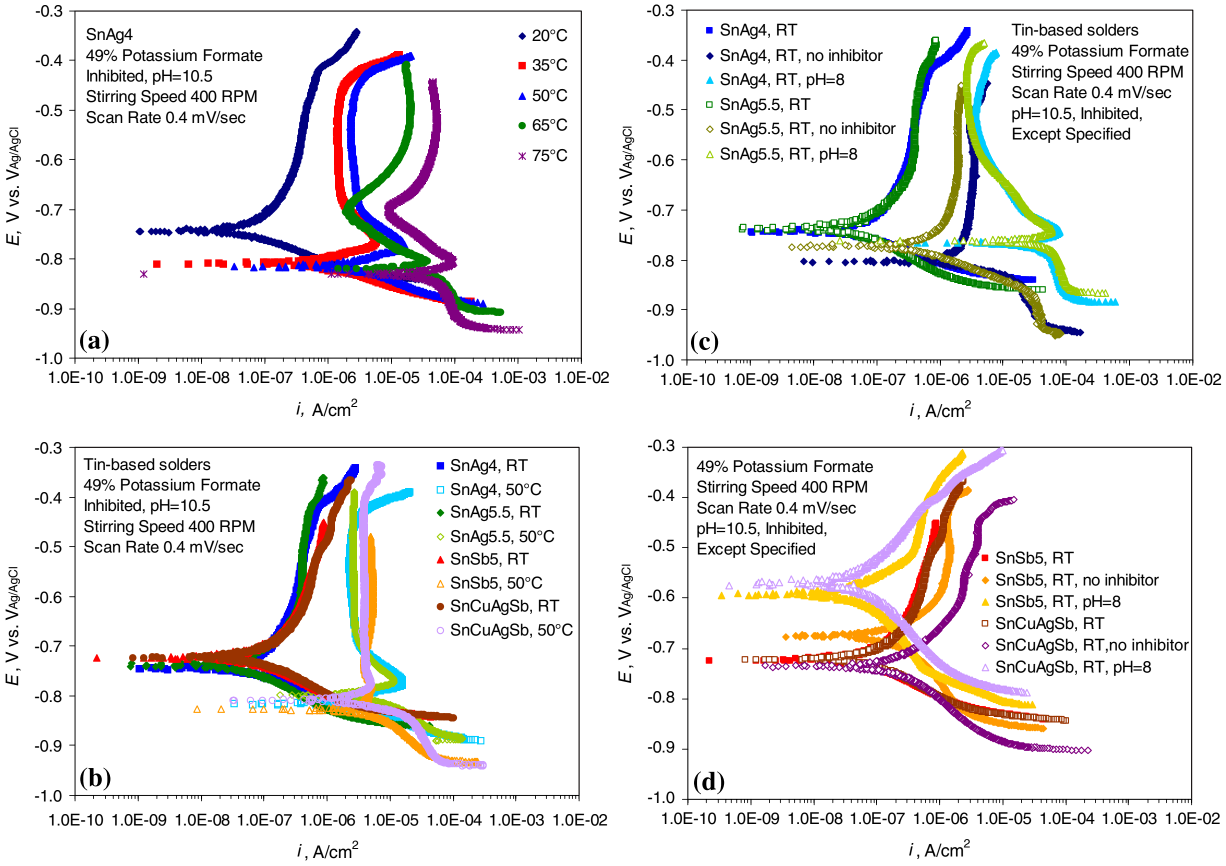

Fig. 3 Potentiodynamic scan curves of (a) SnAg4 in solution #1 at different temperatures; (b) Different tin-based solders in solution #1 at room temperature (RT) and 50 °C; (c) SnAg4 and SnAg5.5, and (d) SnSb5 and SnCu5Ag2Sb2 in different solutions at room temperature

$$(\mathrm{CR})_{\mathrm{copper}} = 1.60 \times 10^{9} \cdot \exp\left[-\frac{5.86 \times 10^{4}}{RT}\right] \ (\mu\mathrm{m/year}), \tag{Eq 2}$$

where R is the universal gas constant (8.31 J K^{-1} mol^{-1}), T is temperature (K), and the energy term was:

$$\Delta E_{\mathrm{solder}} = 105.8\ \mathrm{kJ/mol}, \tag{Eq 3}$$

$$\Delta E_{\mathrm{copper}} = 58.6\ \mathrm{kJ/mol}. \tag{Eq 4}$$

It can be seen that, the effects of temperature in general corrosion rate of the solder were much more significant than in that of copper. For example, according to the Eq. (1) and (2), the corrosion rate of SnAg4 would be 0.94 μm/year at 20 °C and 176.24 μm/year at 60 °C, yet that of copper would be 0.06 μm/year at 20 °C and 1.02 μm/year at 60 °C.

3.4 Galvanic Corrosion of SnAg4 and Copper Couples

Galvanic potential (E_g) and galvanic corrosion rate (calculated from galvanic current) of the solder (SnAg4)-copper couples (tested at an area ratio of A_{SnAg4}:A_{cu} = 0.78) were plotted in Fig. 1b and 2b, respectively. The values of E_g fell between the open-circuit potentials and corrosion potentials of the two materials (Fig. 1b), i.e., lower than E_{oc} and E_{corr} of copper (cathodic), and higher than E_{oc} and E_{corr} of SnAg4 (anodic). The temperature dependence of E_g was similar to that of E_{oc} or E_{corr} of SnAg4.

The temperature dependence of the galvanic corrosion rates of SnAg4 (A_{SnAg4}:A_{cu} = 0.78) can be roughly described as:

$$(\mathrm{CR})_{\mathrm{couple}} = 1.65 \times 10^{12} \cdot \exp\left[-\frac{6.25 \times 10^{4}}{RT}\right] \ (\mu\mathrm{m/year}), \tag{Eq 5}$$

$$\Delta E_{\mathrm{couple}} = 62.5\ \mathrm{kJ/mol}. \tag{Eq 6}$$

It can be seen that the temperature dependence of galvanic corrosion was smaller than that of general corrosion. The galvanic corrosion rates were higher at lower temperatures but lower at higher temperatures, than the general corrosion rates. The fitting lines of the general corrosion rates and the galvanic corrosion rates were crossed at about 65 °C (Fig. 2b). However, the effects of area ratio in galvanic corrosion would have to be investigated. In real soldered joints, the exposed area of solder would be much smaller than that of copper components, so that the anodic (solder) current density could be higher and thus higher-galvanic corrosion rates would result. The active-passive behavior of anode could influence the galvanic corrosion process as well.

3.5 Potential (E)-Current Density (i) curves

Figure 3 showed electrochemical potential (E)-current density (i) curves of solders tested with a potentiodynamic scan rate of 0.4 mV/s at different temperatures. According to the change of *E-i* curves or electrochemical behavior in different solutions, the tested alloys could be divided into two groups according to the *E-i* curves, the tin-silver solders SnAg4 and SnAg5.5 in one group, and SnSb5 and SnCu5Ag2Sb2 in another group.

For SnAg4 specimens tested in solution #1 (pH = 10.5 with inhibitor), the *E-i* curves were generally shifted to higher current density and the corrosion potentials slightly lowered down as temperature increased (Fig. 3a). Passivation was observed almost at all temperatures tested, which became more remarkable at 35 and 50 °C across a region from about −0.68 (E_{pass}, passivation potential) to −0.48 V (E_{br}, break down or pitting potential), and became much smaller at 65 and 75 °C. Corrosion rates were also calculated from the passivation current, which were lower than general corrosion rates at temperatures higher than 50 °C (Fig. 2b). Pitting could happen and grow in the solder specimens as the potential went over E_{br} and broke down the passive film, and pits were visually observed on the specimens tested at 75 °C. Cyclic potentiodynamic polarization tests and further analysis are needed to investigate the pitting behavior.

In solution #1 (pH = 10.5 with inhibitor), all the tin-based solder alloys displayed similar behavior at either room temperature (RT = 20-25 °C) or 50 °C (Fig. 3b). Some difference in passivation between the tin-silver solders and those with antimony and/or copper was observed. The tin-silver solders appeared to have a little lower passivation current density and prominent passive potential (E_{pp}) and critical current density (i_{crit}) at 50 °C.

From the *E-i* curves of the two tin-silver solders at room temperature (Fig. 3c), it can be seen that the curves shifted to higher current density and the corrosion potentials slightly went down, as the solution changed from inhibited (solution #1) to uninhibited (solution #2), or from pH = 10.5 (solution #1) to pH = 8 (solution #3), which means that the tin-silver solders can be more active to corrosion in the solutions without inhibitor or with lower pH. In contrast, SnSb5 and SnCu5Ag2Sb2 appeared to have different behavior than the tin-silver solders, especially in solution #3, of which the current density did not shift much and the corrosion potentials went up as pH changed from 10.5 to 8 (Fig. 3d).

4. Conclusions

(1) Among the potassium formate solutions tested, the one at pH = 10.5 with inhibitor was the best for overall corrosion performance of the tested tin-based solders. In this solution, the general corrosion rates of all the tested solders were outstanding at room temperature and excellent at 50 °C. SnAg4 had a lowest corrosion rate at 50 °C in comparison to other solders.

(2) pH value of the potassium formate solutions had an important impact on the corrosion performance of the tin-silver solders. SnSb5 and SnCu5Ag2Sb2 would perform better than SnAg4 and SnAg5.5 in the solution of pH = 8.

(3) Addition of inhibitor was effective to improve the corrosion performance. However, more effective inhibitor would be needed for applications at higher temperatures, as the corrosion rating of the solders became poor at temperatures higher than 65 °C.

(4) The open-circuit potentials and/or corrosion potentials of all the tested tin-based solder alloys were lower than those of copper. Galvanic corrosion of the solders would occur if coupled or soldered to copper. The galvanic corrosion rates of SnAg4 (tested at an area ratio of A_{SnAg4}:A_{cu} = 0.78) were higher at lower temperatures but lower at higher temperatures (65 °C and above), than the general corrosion rates.

(5) Both the general and galvanic corrosion rates of the solders were increased with temperature. The temperature dependence of corrosion rates of the solders could be described by Arrhenius type equations, and general corrosion had a greater temperature dependence than galvanic corrosion, as shown by the tests of SnAg4.

(6) The electrochemical behavior of the tested solders appeared similar in the solution of pH = 10.5 with inhibitor. However, differences were observed between the tin-silver solders and the ones with antimony and/or copper, especially in the solution of pH = 8.

(7) Passivation was observed at all the solders tested in the solutions of pH = 10.5 with inhibitor, especially at medium temperatures of 35 °C and 50 °C. Pitting was seen on the specimens tested at 75 °C.

References

1. N.C. Lee, Pb-free Soldering–where the World is Going, *Adv. Microelect.*, 1999, **26**(No. 5), p 29–34
2. P. Juul, K. Zachariassen, T. Roslund, S.A. Hansen, L. Ebdrup, B.S. Bentzen, and I.R. Nielsen, "Survey on lead free solder systems", The Danish Environmental Protection Agency, Environmental Project No. 778, 2003
3. J. Glazer, Metallurgy of Low-temperature Pb-free Solders for Electronic Assembly, *Int. Mater. Rev.*, 1995, **40**(No. 2), p 65–93
4. S.K. Kang, P.A. Lauro, D.-Y. Shih, D.W. Henderson, and K.J. Puttlitz, Microstructure and Mechanical Properties of Lead-free Solders and Solder Joints used in Microelectronic Applications, *IBM J. Res. Dev.*, 2005, **49**(No. 4/5), p 607–620
5. V.I. Igoshev and J.I. Kleiman, Creep Phenomena in Lead-free Solders, *J. Electronic Mater.*, 2000, **29**(No. 2), p 244–250
6. Y. Kariya and M. Otsuka, "Mechanical fatigue characteristics of Sn-3.5Ag-X (X = Bi, Cu, Zn and In) solder alloys", *J. Electronic Mater.*, 1998, **27**(No. 11), p 1229–1235
7. K.-W. Moon, W.J. Boettinger, U.R. Kattner, F.S. Biancaniello, and C.A. Handwerker, Experimental and Thermodynamic Assessment of Sn-Ag-Cu solder alloys", *J. Electronic Mater.*, 2000, **29**, p 1122–1236
8. M. Brennen, J.R. Perumareddi, V.S. Sastri, M. Elboujdaini, and J.R. Brown, Studies on Leaching of Metals from Solders Due to Corrosion, *Mater. Corr.*, 1999, **49**(No. 8), p 551–555
9. H. Oulfajrite, A. Sabbar, M. Boulghallat, A. Jouaiti, R. Lbibb, and A. Zrineh, Electrochemical Behavior of a New Solder Materials (Sn-In-Ag), *Mater. Lett.*, 2003, **57**(No. 28), p 4368–4371
10. U.S. Mohanty and K.-L. Lin, Electrochemical corrosion behavior of lead-free Sn-8.5Zn-X Ag-0.1Al-0.5Ga solder in 3.5% NaCl solution, *Mater. Sci. Eng. A*, 2005, **406**(No. 1-2), p 34–42
11. T.C. Chang, M.H. Hon, M.C. Wang, and D.Y. Lin, Electrochemical behaviors of the Sn-9Zn-xAg lead-free solders in a 3.5 wt% NaCl solution, *J. Electrochem. Soc.*, 2004, **151**(No. 7), p C484–C491
12. M. Mori, K. Miura, T. Sasaki, and T. Ohtsuka, Corrosion of tin alloys in sulfuric and nitric acids, *Corr. Sci.*, 2002, **44**(No. 4), p 887–898
13. S.H. Oh, C.B. Bahn, and I.S. Hwang, Evaluation of Thermal Liquid Junction Potential of Water-filled External Ag/AgCl Reference Electrode, *J. Electrochem. Soc.*, 2003, **150**(No. 6), p E321–E328
14. D.A. Jones, Principles and Prevention of Corrosion, 2nd ed., Prentice-Hall, 1996, p 34, 76–88